Optics Communications 524 (2022) 128794

Contents lists available at ScienceDirect

Optics Communications

journal homepage: www.elsevier.com/locate/optcom

Flexible random laser from a porous polymer film

Van Duong Ta [a,*], Duy Tuan Le [a], Thi Lien Ngo [b], Xuan Thau Nguyen [b]

[a] Department of Optical Devices, Le Quy Don Technical University, Hanoi 100000, Viet Nam
[b] Department of Physics, Le Quy Don Technical University, Hanoi 100000, Viet Nam

ARTICLE INFO

Keywords:
Random laser
Thin film
Inverted photonic glass
Flexible
Bendable

ABSTRACT

Flexible random lasers have attracted a great deal of interest due to their potential in light-weight, flexible optical sensors and devices. Among many alternatives, flexible thin film random lasers are very interesting because they can be easily fabricated via a simple solution-based process. Herein, we demonstrate a dye-doped porous polyvinyl alcohol film that can work as a flexible random laser source under optical pumping. The film is fabricated by a drop cast technique and has a nearly circular shape with a diameter of ~5 mm. Owing to the inverted photonic glass structure that is air voids in the polymer matrix, light emission from dye molecules is multiple scattering and lasing emission is achieved. In the central area, the film laser works reliably with the lasing threshold of ~ 166 μJ/mm^2 and lasing wavelength of around 595 nm. In the edge area, the lasing properties are more fluctuated indicating that the structure may not be uniform. It is found that the lasing wavelength in the edge area is 4.5 nm red-shifted compared to that in the central area of the film. Interestingly, the thin film laser can operate well under bending conditions with a minor change in the lasing wavelength.

1. Introduction

Flexible lasers have drawn significant attention due to their potential in lightweight and wearable devices [1,2]. Flexible lasers can be made of various materials and they can be in different forms including sphere [3], disk [4,5], fiber [6] and film [7–10]. Among many alternative structures, film-based lasers are very interesting because they can be fabricated by a simple solution-based process, are easily handled and work well on different substrates [10]. Similar to other kinds of lasers, thin film lasers need an optical cavity for light amplification and a distributed feedback (DFB) cavity is usually used due to its efficiency for in-plane optical feedback [11,12].

Compared to conventional lasers, random lasers are simpler to fabricate because they rely on a highly scattering medium for light amplification without the requirement for an optical cavity [13]. Random lasers have rich physical properties [14] and a wide range of applications including speckle-free laser imaging [15], biosensing [16], bio-integration [17], cancer diagnostics [18] and display [19]. Following the development of flexible film lasers, flexible film random lasers are also emerging owing to their promising applications in flexible sensors and devices [20–30].

Film-based random laser can be realized by various approaches such as embedding active materials in form of nanoparticles [20,21], nanorods [22] in a polymer film. In case the active material cannot be served as a scattering medium then dielectric particles are doped to enhance the light scattering [24]. In addition, metallic particles can also be added to provide local surface plasmon for improved lasing performance [29–32]. Recently, inverted photonic glass (connected air voids in a polymer matrix) has been demonstrated as an excellent scattering structure for random lasers [16,33] but flexible film random lasers based on this structure have not been reported. Developing flexible film random lasers on inverted photonic glass structures is necessary because this structure has some advantages such as simple fabrication via solution process, promising for sensitive sensing applications [16]. As result, this kind of random laser has the potential for lightweight wearable sensors and optical devices. In this work, we present a simple technique to achieve a flexible film (thickness of only 12 μm) random laser using an inverted photonic glass structure as a scattering medium.

2. Experimental methods

2.1. Fabrication of dye-doped porous polymer films

The dye-doped porous film was fabricated from an aqueous suspension that contains polyvinyl alcohol (PVA) polymer serving as a matrix, rhodamine B (RhB) serving as a gain medium and polystyrene (PS) microparticles serving as a template for creating the porous structure. Firstly, 0.5 mL aqueous PVA solution (4 wt%) was mixed with 0.04 mL aqueous RhB solution (1 wt%). Then, 0.2 mL of monodisperse PS microparticles (10 wt%) was added. The final mixture was shaken by a vortex mixer 2 min before use. The PVA (molecular weight of 89

* Corresponding author.
E-mail address: duong.ta@lqdtu.edu.vn (V.D. Ta).

https://doi.org/10.1016/j.optcom.2022.128794
Received 19 March 2022; Received in revised form 14 July 2022; Accepted 16 July 2022
Available online 20 July 2022

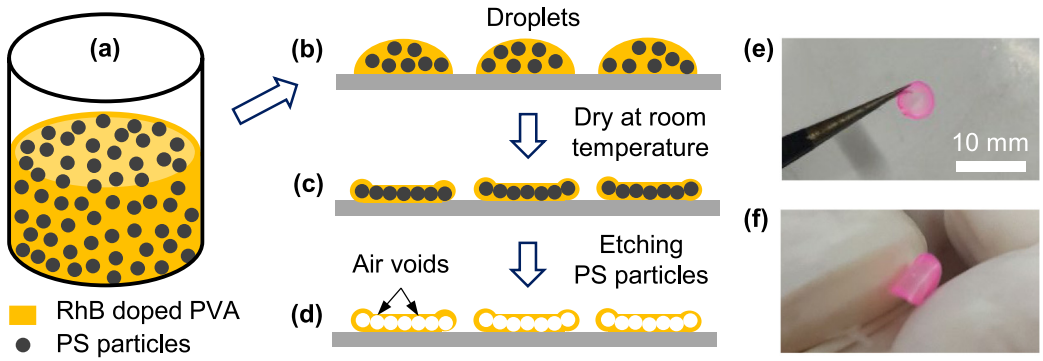

Fig. 1. (a)–(d) Schematic diagram showing the fabrication of porous polymer films. (a) Aqueous suspension contains RhB, PVA and PS particles. (b) Deposition of droplets on a glass substrate. (c) Films structure obtained after the droplets completely dry. (d) RhB-doped porous PVA films achieved by chemically etching the PS particles. (e) and (f) Optical image of RhB-doped PVA film in the straight and bending conditions.

000–98 000) and RhB (dye content 95%) were purchased from Sigma-Aldrich. The PS microparticle with the same diameter of 1.28 μm was purchased from Particles GmbH.

From the above aqueous suspension, porous PVA films were obtained by a simple fabrication process shown in Fig. 1a–d. Firstly, a micropipette was used to take the suspension (Fig. 1a) and subsequently to deposit droplets on a glass substrate (Fig. 1b). The droplet volume was around 10 μL. Then, droplets were left to dry (several hours) at room temperature and in ambient conditions. After drying, film structures with nearly circular shapes are obtained (Fig. 1c). Due to the coffee-stain effect, these films are thicker on the edge and thinner in the central area [34]. Finally, the substrate with the polymer films was immersed in ethyl acetate and left overnight. This solvent etches PS particles but does not affect the polymer thus porous structures are formed (Fig. 1d). A typical dye-doped film with a diameter of around 5 mm is presented in Fig. 1e. It can be seen that the red color in the central area is lighter than on the edge. It is because of the coffee-stain effect that the thickness of the film is thinner in the central area and much thicker on the edge [34]. Especially, owing to its thin thickness, the film is bendable which is potential for flexible optical devices (Fig. 1f).

2.2. Optical characterizations

The dye-doped porous film was investigated by using a micro-Photoluminescence (μ-PL) set up at room temperature and in ambient conditions. This system contains a pump laser, a microscope and a spectrometer. The pumping source was a pulsed Nd: YAG laser (Teem Photonics) with a wavelength of 532 nm and a pulse duration of 400 ps. The pumping laser beam was guided and directed through an objective lens (a magnification of 20×) of a Nikon Eclipse Ti-U inverted microscope to excite the sample. The laser spot was about 80 μm in diameter. Emission from the film was collected through the same objective and coupled to a spectrometer for spectral recording.

3. Results and discussion

3.1. Structure of the dye-doped porous polymer film

The film was cut through its center and then studied by a scanning electron microscope (SEM). From the SEM image, it can be seen that the film is quite thin and flexible (Fig. 2a). The thickness of the film in the central area is about 12–15 μm (Fig. 2b). Due to the coffee-stain effect, it gradually increases in the edge area and reaches a maximum value of ~ 120 μm (Fig. 2c). The porous structure is visible throughout the film cross-section. As the PS microparticles are closely packed, the air voids are expected to be well connected. This expectation is confirmed in the high magnification SEM image where air voids are connected and distributed uniformly (Fig. 2d). This structure is called inverted photonic glass and has been demonstrated as a highly scattering medium for the realization of random lasing emission [16].

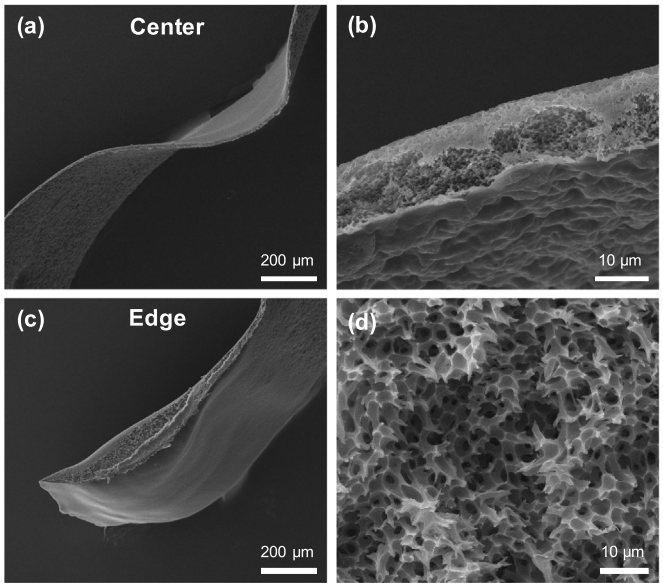

Fig. 2. (a) and (b) SEM and close-up SEM images of the cross-section of a porous polymer film in the central area. (c) SEM image of the cross-section on the edge of the film. (d) High magnification SEM image showing the porous structure with the air voids.

3.2. Random lasing emission from the central area of the film

The dye-doped porous films can work as efficient random lasers under optical pumping.

Under optical excitation, light emission from dye molecules (embedded in the polymer) is scattered many times between the polymer-air interface (Fig. 3a). This process leads to light amplification and subsequently lasing emission is obtained. Since the thickness of the film in the central and the edge area are different, we will study them separately and then make a comparison.

In the center of the film, as shown in Fig. 3b, the development from spontaneous to stimulated emission can be observed clearly. Under the pump pulse fluences (PPF) smaller than 115 μJ/mm^2, the emission intensity is weak and the spectrum is broad which is the characteristic of spontaneous emission. At PPF of 115 μJ/mm^2, the emission intensity increases sharply and the spectrum becomes much narrower, indicating evidence of stimulated emission. At this PPF, it can be said that the optical gain is higher than the loss thus the threshold is reached for some random lasing mode. However, the lasing mode is not clear herein as the emission curve is still quite smooth. Lasing mode only appears clearly when the pump fluence is much larger. As a result, the easier

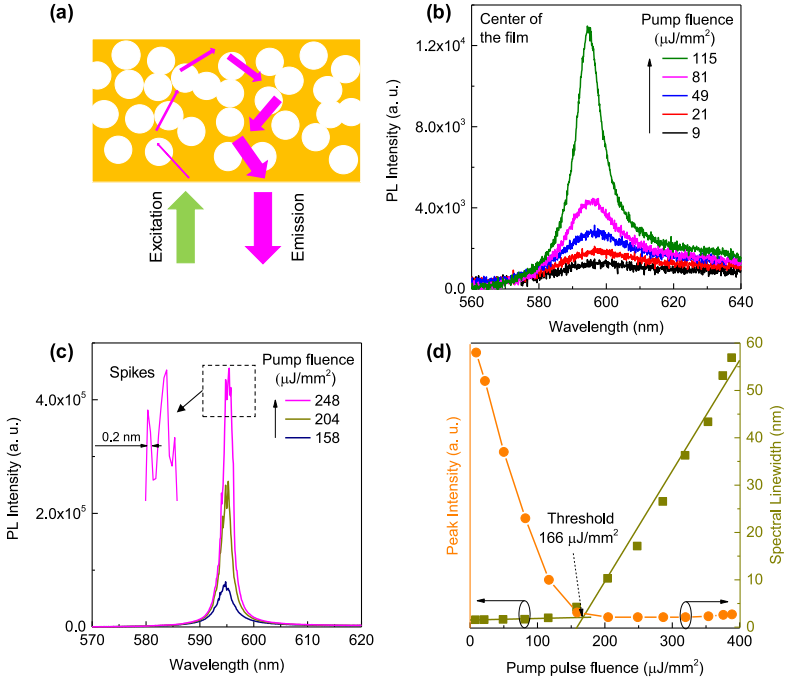

Fig. 3. (a) Schematic of light amplification via multiple scattering in a porous film. (b) and (c) Emission spectra from the center of the film under various pump pulse fluences. (d) Corresponding PL peak intensity and spectral linewidth of the emission from the film as a function of pump fluences.

way to determine the threshold is by plotting the emission intensity with PPF and then finding the inflection point, which will be discussed later.

The stimulated emission increases with increasing PPF. When PPF is higher than 115 μJ/mm^2, lasing emission with central wavelength at 595.3 nm is dominant, indicated by a very high emission intensity and narrow spectrum (Fig. 3c). Especially, some spikes with spectral linewidth down to 0.2 nm (limited by the spectral resolution of our spectrometer) are observed.

To determine the lasing threshold, peak emission intensity is plotted as a function of PPF (Fig. 3d). As the pumping fluence increases, the output emission intensity increases gradually until a sudden rise which indicates a distinct lasing threshold of 166 μJ/mm^2. This value is comparable to several flexible random dye lasers (threshold of 133 μJ/mm^2 [29]) but it is still higher compared with some dye-doped flexible random lasers (threshold of 2.87 mJ/cm^2 [28]). To reduce the lasing threshold, the dye concentration and the size of air voids need to be optimized which is worth investigating in future work.

In addition, the chance of the spectral linewidth of the emission is also consistent with the change in the emission intensity. As shown in Fig. 3d, the spectral linewidth decreases almost linearly with increasing pumping energy until the threshold value. Starting from around 60 nm, the spectral linewidth decreases to about 3 nm at the threshold. It goes down to about 2 nm and maintains at this value for higher pumping fluences.

In comparison with conventional lasers, the lasing performance of the thin film random laser in terms of lasing threshold and quality factor of lasing mode may not be as good as flexible lasers based on whispering gallery mode [4,5], DFB [10] and Fabry–Perot cavity [35]. However, this thin film random laser has some advantages over traditional lasers such as simpler fabrication, less sensitivity to the structure defect (it can work well even broken down to small pieces) and especially they can be used as illuminated sources for speckle-free imaging [15].

3.3. Random lasing emission from the edge of the film

Similar to the center of the film, lasing emission is also observed from the edge of the film where the thickness is the highest. As shown in Fig. 4a, the evolution from spontaneous emission to stimulated and lasing emission can be seen clearly. The central wavelength of the lasing emission is 599.9 nm and the lasing threshold is determined to be 119 μJ/mm^2 (Fig. 4b). Compared with the lasing characteristics from the center of the film, the emission from the edge is red-shifted (~4.5 nm) and the lasing threshold is lower. However, lasing characteristics can be varied at different positions of the film thus more positions are needed to study for a reasonable comparison.

3.4. Comparison of lasing characteristics of various positions in the film

To compare the lasing properties between the central and edge area of the film, we investigated various positions in these areas. These positions were randomly chosen all over the studied area as schematically shown in Fig. 5a. It can be seen that the lasing thresholds in different positions in the central area are very similar, are around 166 μJ/mm^2. The threshold variation is small, less than 2%, indicating that the structure in the central area is quite uniform. In contrast, the lasing threshold in the edge area fluctuates largely from 119 to 206 μJ/mm^2. The thickness varies more dramatically in the edge area thus the threshold fluctuation may be related to the thickness variation. However, on average, the lasing threshold difference between the central and edge area is not high. In the central area, the average lasing threshold is 166 μJ/mm^2 while it is slightly lower (162 μJ/mm^2) on the edge. As a result, it is suggested that the variation in the internal structure may have a stronger influence on the threshold fluctuation than the thickness variation. The porous structure in the central area is supposed to be uniform. However, it may not be very uniform in the edge because the edge is formed by the coffee-stain effect which is strongly affected by surrounding temperature and humidity. In addition, the local surface inclination of the film may also induce fluctuation. All these issues will be studied in future work.

Not only the lasing threshold but the laser wavelength of the edge area is also more fluctuated compared with that of the central area (Fig. 5c). In the edge area, the variation from the shortest wavelength (599.4 nm) to the longest wavelength (601.8) is 2.4 nm. This value is 3 times higher compared with 0.8 nm (from 594.9 to 595.7 nm) in the central area. In addition, there is a distinct difference in the

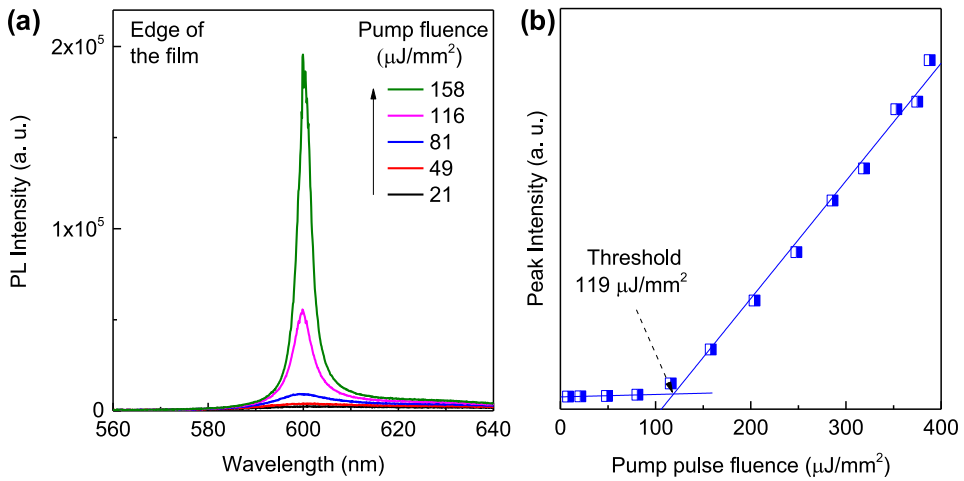

Fig. 4. (a) Emission spectra from the edge of the film under various pump pulse fluences. (b) Corresponding PL peak intensity as a function of pump fluences.

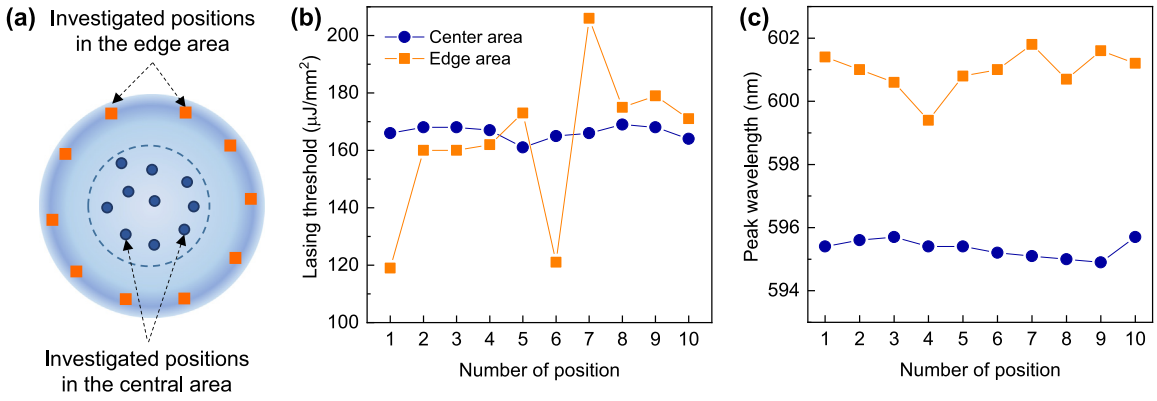

Fig. 5. (a) Schematic of randomly investigated positions in the film. (b) and (c) Lasing threshold and peak wavelength at different positions in the central and edge area of the film.

lasing wavelength between the two areas. The lasing wavelength in the edge area is generally red-shifted (~4.5 nm) compared with that in the central area. This phenomenon is common and is related to the thickness of the film. On the edge, the thickness is much larger than that in the central area thus light travels a longer path before scattering out, therefore, it has a higher possibility to be reabsorbed by the dye molecules [33]. Shorter wavelengths are being reabsorbed more than longer wavelengths leading to the red-shift of the lasing emission in the edge area.

Overall, the result indicates that lasing properties in the central area are nearly the same which is not dependent on the pumping position. In other words, this film laser works reliably in the central area. On the edge of the film, the lasing threshold is more fluctuated between different positions but the lasing wavelength is quite similar, showing a variation of ~2.4 nm. Since the lasing wavelength in the central and edge area are varied, it provides the optional wavelength for a specific use.

3.5. Random lasing emission from a bending film

Owing to the thin structure and flexibility of the PVA polymer, the porous film laser can be easily bended. Theoretically, the spherical air voids in the normal form will change to ellipsoidal air voids upon bending and this effect may lead to some changes in the lasing threshold and wavelength. To study this effect, we monitored the lasing threshold and wavelength while bending the film. We use the radius of curvature (R) to quantitatively characterize the bending effect. We did not observe a clear wavelength shift until the R downs to 1.8 cm as schematically shown in the inset of Fig. 6a. At this condition, the lasing threshold obtained is 243 μJ/mm^2 which is higher than 166 μJ/mm^2 of the straight film (Fig. 6a). In other words, the threshold has increased by about 46% under the bending condition. Fig. 6b indicates that the bending film can work well and its lasing emission is slightly blue-shifted compared with that of the straight film. After release, the film can come back to its straight form and work normally. In addition, we have tested the repeatability of the bending measurement and found that the lasing wavelength shift is only observed in the first two or three times of measurements. After that, the wavelength is near unchanged under bending conditions.

For R smaller than 1.8 cm, the film can be broken or cannot come back to its original straight form thus we did not study this case. For better mechanical flexibility, it is worth making lasers with a larger area and thinner thickness. In addition, the variation of mechanical properties and lasing performance of the thin films with increasing the molecular weight of PVA would also be interesting and we will consider studying it in future work.

4. Conclusion

We have demonstrated a flexible thin film random laser fabricated by a simple solution-based process. The lasing mechanism is based on light scattering in porous inverted photonic glass structures distributed all over the film. The lasing properties including lasing threshold and lasing wavelength are investigated in the central area and edge of the film. In the central area, this film laser works reliably with the lasing threshold of ~166 μJ/mm^2 and lasing wavelength at peak intensity

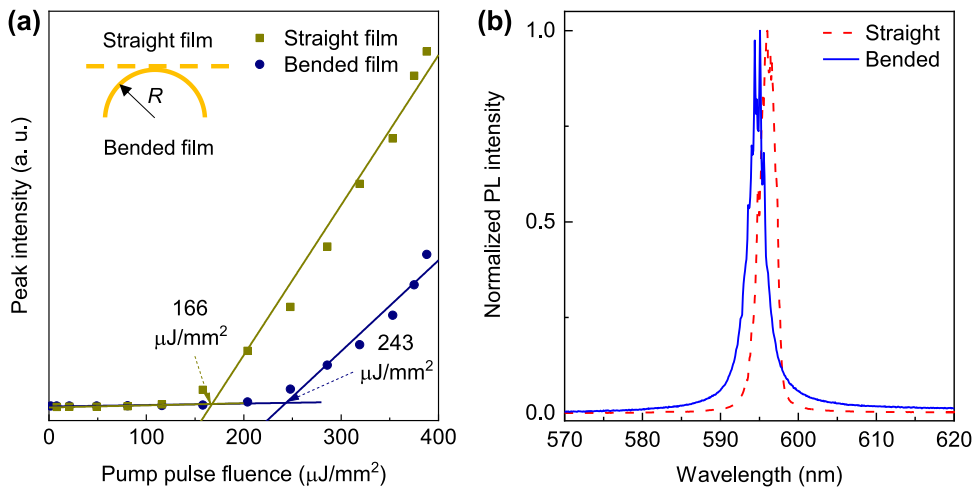

Fig. 6. (a) PL peak intensity of the straight and bended film laser as a function of pump fluences. The inset presents a schematic curvature of the straight and bended thin film. Radius of the curvature (R) is about 1.8 cm. (b) Emission spectra of the film at the straight and bending conditions.

of ~595 nm. In the edge area, the lasing threshold more fluctuates from position to position but the lasing wavelength is quite similar. In addition, due to a larger thickness, the lasing wavelength in the edge area is 4.5 nm red-shifted compared to that in the central area. Especially, the thin film laser can work well under bending conditions with a slight change in the lasing wavelength. Our work is meaningful for the development of ultra-thin random lasers which can be potential in wearable sensors and devices.

Declaration of competing interest

The authors declare that they have no known competing financial interests or personal relationships that could have appeared to influence the work reported in this paper.

Data availability

Data will be made available on request.

Acknowledgments

This research is funded by Le Quy Don Technical University, Viet Nam under grant number 20.1.029. The authors thank Mr Nguyen Minh Hoang for assistance in the sample fabrication and professor Riccardo Sapienza, Imperial College London, for the support in optical characterizations.

References

[1] V.D. Ta, Y. Wang, H. Sun, Microlasers enabled by soft-matter technology, Adv. Opt. Mater. 7 (2019) 1900057.
[2] I.D.W. Samuel, Laser physics: Fantastic plastic, Nature 429 (2004) 709–711.
[3] V.D. Ta, R. Chen, H.D. Sun, Tuning whispering gallery mode lasing from self-assembled polymer droplets, Sci. Rep. 3 (2013) 1362.
[4] T. Zhou, K.W. Ng, X. Sun, Z. Zhang, Ultra-thin curved visible microdisk lasers with three-dimensional whispering gallery modes, Nanophotonics 9 (2020) 2997–3002.
[5] C. Zhang, H. Dong, C. Zhang, Y. Fan, J. Yao, Y.S. Zhao, Photonic skins based on flexible organic microlaser arrays, Sci. Adv. 7 (2021) eabh3530.
[6] R. Chen, V.D. Ta, H.D. Sun, Bending-induced bidirectional tuning of whispering gallery mode lasing from flexible polymer fibers, ACS Photonics 1 (2014) 11–16.
[7] S. Schauer, X. Liu, M. Worgull, U. Lemmer, H. Hölscher, Shape-memory polymers as flexible resonator substrates for continuously tunable organic DFB lasers, Opt. Mater. Express 5 (2015) 576–584.
[8] A.S.D. Sandanayaka, T. Matsushima, F. Bencheikh, K. Yoshida, M. Inoue, T. Fujihara, K. Goushi, J.-C. Ribierre, C. Adachi, Toward continuous-wave operation of organic semiconductor lasers, Sci. Adv. 3 (2017) e1602570.
[9] J.R.C. Smirnov, A. Sousaraei, M.R. Osorio, S. Casado, J.J. Hernández, L. Wu, Q. Zhang, R. Xia, D. Granados, R. Wannemacher, I. Rodriguez, J. Cabanillas-Gonzalez, Flexible distributed feedback lasers based on nanoimprinted cellulose diacetate with efficient multiple wavelength lasing, npj Flex. Electron. 3 (2019) 17.
[10] M. Karl, J.M.E. Glackin, M. Schubert, N.M. Kronenberg, G.A. Turnbull, I.D.W. Samuel, M.C. Gather, Flexible and ultra-lightweight polymer membrane lasers, Nature Commun. 9 (2018) 1525.
[11] M.D. McGehee, M.A. Dıaz-Garcıa, F. Hide, R. Gupta, E.K. Miller, D. Moses, A.J. Heeger, Semiconducting polymer distributed feedback lasers, Appl. Phys. Lett. 72 (1998) 1536–1538.
[12] P. Görrn, M. Lehnhardt, W. Kowalsky, T. Riedl, S. Wagner, Elastically tunable self-organized organic lasers, Adv. Mater. 23 (2011) 869–872.
[13] D. Wiersma, Laser physics: The smallest random laser, Nature 406 (2000) 132–135.
[14] F. Luan, B. Gu, A.S.L. Gomes, K.-T. Yong, S. Wen, P.N. Prasad, Lasing in nanocomposite random media, Nano Today 10 (2015) 168–192.
[15] B. Redding, M.A. Choma, H. Cao, Speckle-free laser imaging using random laser illumination, Nature Photon. 6 (2012) 355.
[16] S. Caixeiro, M. Gaio, B. Marelli, F.G. Omenetto, R. Sapienza, Silk-based biocompatible random lasing, Adv. Opt. Mater. 4 (2016) 998–1003.
[17] V.D. Ta, T.T. Nguyen, T.H.L. Nghiem, H.N. Tran, A.T. Le, N.T. Dao, P.D. Duong, H.H. Mai, Silica based biocompatible random lasers implantable in the skin, Opt. Commun. 475 (2020) 126207.
[18] R.C. Polson, Z.V. Vardeny, Random lasing in human tissues, Appl. Phys. Lett. 85 (2004) 1289–1291.
[19] T.-L. Shen, H.-W. Hu, W.-J. Lin, Y.-M. Liao, T.-P. Chen, Y.-K. Liao, T.-Y. Lin, Y.-F. Chen, Coherent Förster resonance energy transfer: A new paradigm for electrically driven quantum dot random lasers, Sci. Adv. 6 (2020) eaba1705.
[20] S.P. Lau, H. Yang, S.F. Yu, C. Yuen, E.S.P. Leong, H. Li, H.H. Hng, Flexible ultraviolet random lasers based on nanoparticles, Small 1 (2005) 956–959.
[21] X. Shi, Y.-M. Liao, H.-Y. Lin, P.-W. Tsao, M.-J. Wu, S.-Y. Lin, H.-H. Hu, Z. Wang, T.-Y. Lin, Y.-C. Lai, Y.-F. Chen, Dissolvable and recyclable random lasers, ACS Nano 11 (2017) 7600–7607.
[22] T.-M. Sun, C.-S. Wang, C.-S. Liao, S.-Y. Lin, P. Perumal, C.-W. Chiang, Y.-F. Chen, Stretchable random lasers with tunable coherent loops, ACS Nano 9 (2015) 12436–12441.
[23] Y.-M. Liao, Y.-C. Lai, P. Perumal, W.-C. Liao, C.-Y. Chang, C.-S. Liao, S.-Y. Lin, Y.-F. Chen, Highly stretchable label-like random laser on universal substrates, Adv. Mater. Tech. 1 (2016) 1600068.
[24] L. Ye, Y. Feng, Z. Cheng, C. Wang, C. Lu, Y. Lu, Y. Cui, Coherent random lasing from dye aggregates in polydimethylsiloxane thin films, ACS Appl. Mater. Interfaces 9 (2017) 27232–27238.
[25] Y.-C. Wang, H. Li, Y.-H. Hong, K.-B. Hong, F.-C. Chen, C.-H. Hsu, R.-K. Lee, C. Conti, T.S. Kao, T.-C. Lu, Flexible organometal–halide perovskite lasers for speckle reduction in imaging projection, ACS Nano 13 (2019) 5421–5429.
[26] Y. Bian, H. Xue, Z. Wang, Programmable random lasing pluses based on waveguide-assisted random scattering feedback, Laser Photonics Rev. 15 (2021) 2000506.
[27] I.B. Dogru-Yuksel, C. Jeong, B. Park, M. Han, J.S. Lee, T.-i. Kim, S. Nizamoglu, Silk nanocrack origami for controllable random lasers, Adv. Funct. Mater. 31 (2021) 2104914.
[28] G. Dai, L. Wang, L. Deng, Flexible random laser from dye doped stretchable polymer film containing nematic liquid crystal, Opt. Mater. Express 10 (2020) 68–75.

[29] Y.-J. Lee, C.-Y. Chou, Z.-P. Yang, T.B.H. Nguyen, Y.-C. Yao, T.-W. Yeh, M.-T. Tsai, H.-C. Kuo, Flexible random lasers with tunable lasing emissions, Nanoscale 10 (2018) 10403–10411.
[30] K. Ge, D. Guo, X. Ma, Z. Xu, A. Hayat, S. Li, T. Zhai, Large-area biocompatible random laser for wearable applications, Nanomaterials 11 (2021) 1809.
[31] E. Heydari, I. Pastoriza-Santos, L.M. Liz-Marzán, J. Stumpe, Nanoplasmonically-engineered random lasing in organic semiconductor thin films, Nanoscale Horiz. 2 (2017) 261–266.
[32] J.-H. Hsiao, S.-W. Chen, B.-Y. Hung, K. Uma, W.-C. Chen, C.-C. Kuo, J.-H. Lin, Resonant energy transfer and light scattering enhancement of plasmonic random lasers embedded with silver nanoplates, RSC Adv. 10 (2020) 7551–7558.
[33] V.D. Ta, S. Caixeiro, D. Saxena, R. Sapienza, Biocompatible polymer and protein microspheres with inverse photonic glass structure for random micro-biolasers, Adv. Photonics Res. 2 (2021) 2170025.
[34] V.D. Ta, R. Carter, E. Esenturk, C. Connaughton, J. Stringer, P.J. Smith, T. Wasley, J. Li, R. Kay, J. Shephard, Dynamically controlled deposition of colloidal nanoparticles suspension in evaporating drops using laser radiation, Soft Matter 12 (2016) 4530–4536.
[35] A. Camposeo, F. Di Benedetto, R. Stabile, A.A.R. Neves, R. Cingolani, D. Pisignano, Laser emission from electrospun polymer nanofibers, Small 5 (2009) 562–566.